4th International Symposium on Materials and Sustainable Development ISMSD2019
November 12-14, 2019
Boumerdes - Algeria

Effect of Different Anodizing Bath on Improving the Corrosion Resistance of a 2030 Aluminum Alloy

Mm. M. BEN MOHAMED[1, 2], Pr. A. BEN MOUNAH[1], Dr. A. HADDAD[2]

[1.] *University M'hamedBougara, Faculté des Sciences de l'Ingénieur (Campus ouest – Boumerdès) Cité Frantz. Fanon, 35000 Boumerdès, ALGERIE.*
[2.] *Research Center in Industrial Technologies CRTI, BP 64, Route de Dely Brahim, Chéraga, Alger 16014, ALGERIE.*
Email: manel.b92@yahoo.com

***Abstract*— Aluminum alloys have a considerable appeal for mechanical and building designers. This characteristic lies in the mechanical and physicochemical properties of these alloys. Aluminum is often used in the anodized surface condition to impart pleasing aesthetics, higher corrosion resistance, better scratch and wear resistance, and thus an improved value of the product. Anodization is commonly produced by direct current (DC) that offers excellent protection against wear and corrosion. This work focuses on the surface condition of a 2030 aluminum alloy treated with chromium and sulfuric acid. Our goal is to understand what happens at the surface of the Al alloy after each treatment (chromic anodizing, sulfo-chromic anodizing) using a structural characterization (MEB) that will be followed by electrochemical characterization. The results obtained have shown the effectiveness of chromic anodizing, which gives rise to the formation of a thin layer and offers excellent protection against corrosion. Chromic anodic oxidation protects an aluminum part by creating a layer of alumina Al_2O_3, to give it anti-corrosion, decorative and heat resistance characteristics, as well as, any chromic acid residues do not attack the base material. This is the opposite of sulfuric acid, which makes it an excellent pretreatment for aerospace parts.**

***Keywords*— Corrosion; chromic anodizing; sulfo-chromic anodizing; electrochemical characterization; structural characterization.**

1. INTRODUCTION

Aluminum in its natural state is protected by a layer of superficial alumina when it's exposed to the atmosphere, however, when the metal is exposed to a polar environment/ solvent (water or alcohol) or electrolyte solution (salt, acid or alkalin dissolved in water) the surface of the metal acquires an electric potential, which forces the metal ions to leave the metal and move towards the solution as cations. This phenomenon is the mechanism of corrosion of a metal in the presence of electrolyte (seawater) (Laleh et al. 2019).

Aluminum and some alloying elements such as Mg and Zn are very active with very negative standard reduction potentials for their corresponding ions. They react instantly with O_2 to form passivating metal oxide films (Wang et al. 2019). High strength and high resistance is found in 2000 series such as Al-Cu-Mg (AA2024) and Al-Cu-Mg-Pb (AA2030) alloys, which result from alloying elements such as copper and they are widely used in the aeronautic field (Ashtiani and Shahsavari. 2016), they have a low resistance to corrosion and are sensitive to localized corrosion (Jensen et al. 2019; Zhang and Zu. 2019).

Several methods used to improve protectively aluminum and its alloys such as anodizing process, it consists of electrolysis in the middle of an electrolyte, from which the coating is not carried out by adding material but by controlled oxidation of the substrate in order to passivate it (Ma et al. 2020). Anodization is the treatment which often subjected to this alloy, as long as it provides a thick alumina layer that offers decorative appearance, higher corrosion resistance, enhanced scratch and wear resistance, thereby improving the value of the product (Saeedikhani et al. 2017). This treatment is an electrochemical conversion process that forms barrier-type oxide layers or self-organized nonporous/nanotu -bular structures, the morphology of the anodic layer is mainly controlled by the voltage/current in this process (Fadillah et al.2019).

A highly decorative anodic film, which often is obtained by Direct Current (DC) anodizing in chromic or/and sulphuric acid, is greatly influenced by the anodizing parameters as well as the alloy composition, microstructure, and surface morphology. The electrochemical conversion of aluminum to aluminum oxide layer offers a better adhesion of alumina formed on the base material.

Sulfuric Anodic Oxidation (SAO) effectively protects lightweight alloys against corrosion, this process makes it possible to obtain thick layers (Moon et al. 2011). The anodic oxidation takes place in a dilute sulfuric acid bath and electrolytically consists of informing on the surface a layer of alumina which is the result of the combination of aluminum and oxygen released (Nettikaden et al. 2012).

Chromatic Anodic Oxidation process (CAO) results in the formation of a thin layer order of microns thick, but it offers excellent protection against corrosion. Among the advantages of this anodizing is a small thickness of the layer formed, a good rubbing ability (Elabar et al. 2015).

During anodizing treatment, a large number of fine pores

appear in the anodizing layer (Lee and Park. 2014). This superficial porosity impairs the reactivity of the surface with the surrounding environment. This end resulted from the loss of aluminum cations to the electrolyte with reduced growth efficiency close to 60% for the porous film (Fadillah et al. 2019).

The effect of corrosion on the fatigue properties of aluminum alloys is studied in the field of accelerated corrosion tests in NaCl (De Bonfils-Lahovary et al. 2019; Tao et al. 2010).

After the accelerated corrosion of A2024 by 3.5% NaCl, a calculation model has been established which makes the link between the fatigue life before corrosion and the initial state of rupture, concluded that it was not reasonable to directly deduct the pores of corrosion in the form of superficial cracks (Zhang et al. 2019).

Electrochemical techniques have been used to study the corrosion resistance of anodized aluminum alloys. The Electrochemical Impedance Spectroscopy (EIS) technique could characterize the properties of the barrier layer and the sealed porous layer by adapting the impedance spectra to a suitable electrical equivalent circuit. Electrochemical data obtained from the EIS technique could also be used to calculate the thickness of oxide films (Tao et al. 2009; Saeedikhani et al. 2017; Zhang et al. 2019).

Cyclic voltammetry (CV) is a technique that makes it possible to understand the complete behavior of a system, both thermodynamically and kinetically. It is the most widely used method for obtaining information about the electrochemistry of the systems, it consists of sweeping the potential over time and recording the current with respect to the potential (Palagonia et al. 2019).

The anodized layer is made of aluminum from the substrate and oxygen exiting the solution and is not very harmful to the environment. In solution, in an industrial environment, the solution is easily neutralized by caustic soda, producing sodium sulfate.

Chromic Anodic Oxidation (CAO) and Sulfuric Anodic Oxidation (SAO) consist of controlled oxidation of the substrate in an acid medium, these two processes differ in the type of acid used for the anodic oxidation (sulfuric for SAO and chromic for CAO).

In the present study, the anodizing of A2024 alloy with sulfuric acid (SAO) was studied for the first time. The results were compared in the first with that offer by anodizing of A2024 alloy with chromic acid (CAO), then, with that anodizing with sulfo-chromic acid (SCAO). The latter realized under the same condition of working. Finally, all this manipulation will be compared with that of 2024 pure aluminum, for a better understanding of the growth mechanism of the anodic films. Optimal experimental conditions were determinate to obtain films with a good anticorrosive performance in simulated physiological solution.

Before immersion in the electrolyte solution, surface preconditioning by mechanical pretreatment and degreasing is more commonly applied to organic contaminants, which are also typically part of the industrial manufacturing processes.

2. EXPERIMENTAL

2.1 Material and surface pretreatment

TABLE I: The chemical composition of the samples

Elements	Cu	Mg	Mn	Si	Fe	Zn	Ti	Cr
Percentage (%)	7.27	1.46	0.66	0.06	0.21	0.09	0.04	0.017

The samples used in this work are A2024 aluminum alloys with a chemical composition mentioned in the table I. They were used for the measurement of electrochemical with a dimension of $1cm^2$, sealed by epoxy resin and was attached with copper wire. The surfaces of the samples were wet ground up to 1000 grit SiC abrasive papers and cleaned with deionized water and acetone, finally dried with fresh airflow.

Atomic emission plasma spectroscopy revealed by the following composition of AA2024-T3 alloy, knowing that aluminum has a significant percentage by weight of 90%.

2.2 Anodizing treatment

The test solutions were prepared in the first bath with the dilution of 30% concentrated sulfuric acid and bidistilled water, the second bath contains 10% chromic acid and double distilled water, the last bath is the mixture of the two previous acids. The treatment time is 30 minutes at a temperature of 50 °C, an undercurrent of 2 à A/dm^2 and stirring at a low speed. Once the anodization cycle is complete, electrochemical characterization is done in a solution that contains 3.5% NaCl. Every experience was repeated twice and the average value was reported in order to reach reproducibility of results.

2.3 Characterizations of oxide layer and corrosion products

For the characterization of oxide layers formed after treatment and corrosion products, scanning electron microscopy (SEM) and energy dispersive X-ray (EDS) spectrum analysis are required. Before the observations with SEM, the samples were covered with a thin aluminum film to increase the electro-conductivity of the sample that was hoisted with a resin.

2.4 Electrochemical measurement

For this anodization and for the electrochemical tests we used a five orifice cell from the solution, the temperature (T) and three electrodes are the Ag/AgCl reference electrode (RE), the platinum counter electrode (CE) and finally the aluminum A2024 alloy working electrode (WE). The working electrode (WE) was immersed in an aggressive solution for a few minutes before open circuit potential (OCP), to obtain a more stable potential in electrochemical test. The impedance measurements were transmitted in the frequency range from 100 kHz to 10 MHz with an AC amplitude signal of 10 mV (RMS). Cyclic voltammetry (single) was performed with a balancing potential between -1V/1V and ended with the same potential, with a scan rate of 0.01V / S.

3. ANODIZING REACTION

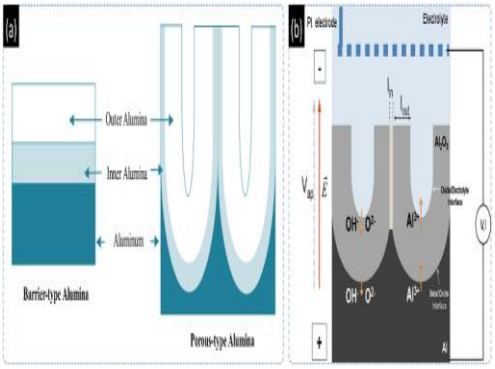

Fig. 1. Schematic diagrams showing elementary interfacial reactions for (a) barrier-type and (b) porous-type anodic oxide (Sousa et al. 2014).

Anodizing can be presented by a series of reactions:

• Cathode: $2H^+ + 2e^- \rightarrow H_2$ (1)

• Anode: $Al \rightarrow 3e^- + Al_3^+$ (2)

Then: $2Al_3^+ + 3H_2O \rightarrow Al_2O_3 + 6H^+$ (3)

Balance equation: $2Al + 3H_2O \rightarrow Al_2O_3 + 3H_2$ (4)

Reactions 2, 3 and 4 correspond to the formation of anodic oxide at the metal/electrolyte interfaces, respectively. These reactions thus cause a formation of an aluminum oxide layer which isolates the electric current arriving at the layer (Sousa et al. 2014).

The pore walls are composed of pure alumina in the regions furthest from the pore (inner layer) and alumina contaminated with anions (outer layer) just next to the nanopore (Bai et al. 2004). It's shaw in Fig. 1.

Corrosion can be presented by a series of reactions:

$$Al_2O_3 + 6H^+_{(aq)} \rightarrow 2Al^{3+}_{(aq)} + 3H_2O_{(l)} \quad (5)$$

$$Al_2O_3 + nH_2O_{(l)} \rightarrow 2Al^{3+}_{(aq)} + (3- n- x)O^{2-}_{(ox)} + xOH^-_{(ox)} + (2n-x)\,3H^+_{(aq)} \quad (6)$$

Reaction 5 describes the dissolution of the alumina layer by Joule heat-induced oxide dissolution and/or field-induced oxide dissolution, where n represents the amount of dissociated water per mole of Al2O3 dissolved at the same time (Lee and Park. 2014).

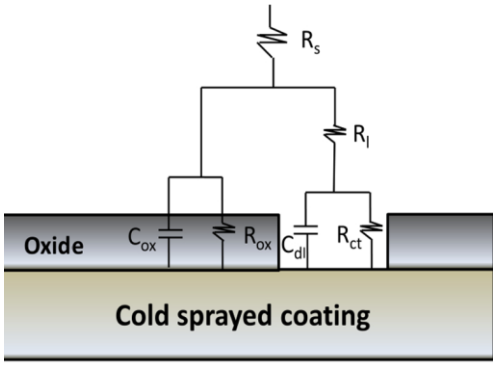

Fig. 2. Schematic representation of the corrosion process and the proposed equivalent circuit from cross-sectional view (Zhang et al. 2019).

The heterogeneous microstructure of high strength aluminum alloys and metal matrix composites (MMC) are sensitive to localized corrosion, such as corrosion of cracks, crevices, intergranular and exfoliation (Datta et al. 2008), an example of this phenomenon is shown in Fig. 2. Corrosion of the aluminum sample caused mainly by the presence of chloride ions (presented in solution aggressive NaCl), which causes the decreased durability of aluminum structures.

4. RESULTS AND DISCUSSION

4.1 Electrochemical polarization and impedance measurements.

To investigate the corrosion behavior of 2024 aluminum alloy in 3.5% NaCl with anodizing in different acids bath, the electrochemical polarization was performed and the polarization curves of the plot were shown in Fig. 3. The representation of NYQUIST in Sulfuric anodizing (SAO) has at high and low frequency a well defined capacitive loop and an inductive loop badly separated from the first one, this could be due to the desorption of corrosion products or due to the desorption of Cl^-/corrosion products (Liu et al. 2016).

Almost the same behavior for chromic anodic oxidation (CAO) is it represented in the same figure, but with great resistance, this high resistive value corresponds to the passivation of the anodic layer of the metal or it is called polarization resistor. On the other hand, in the case where the material is treated with sulfo-chromic anodic oxidation (SCAO) one observes a large capacitive loop but which ends with diffusion, this diffusion shows that the oxide layer produced during the anodizing treatment (SCAO) is less compact, therefore less adherent in has a low frequency which means that corrosion reached the base metal.

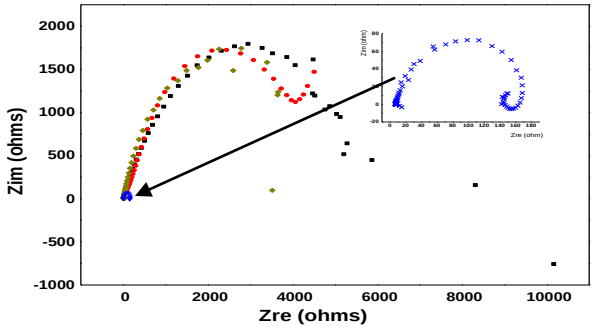

Fig. 3. The impedance curve of AA 2024 treated with different anodizing baths in aerated 3,5% NaCl solution. ■ CAO, ● SCAO, ♦ Al, x SAO.

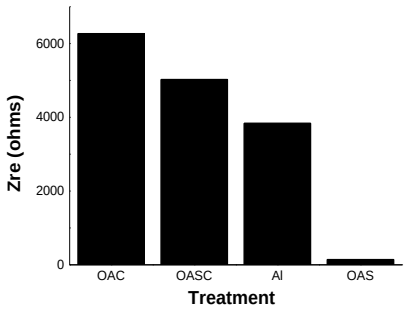

Fig. 4. The Impedance diagram according to the deferent treatments baths.

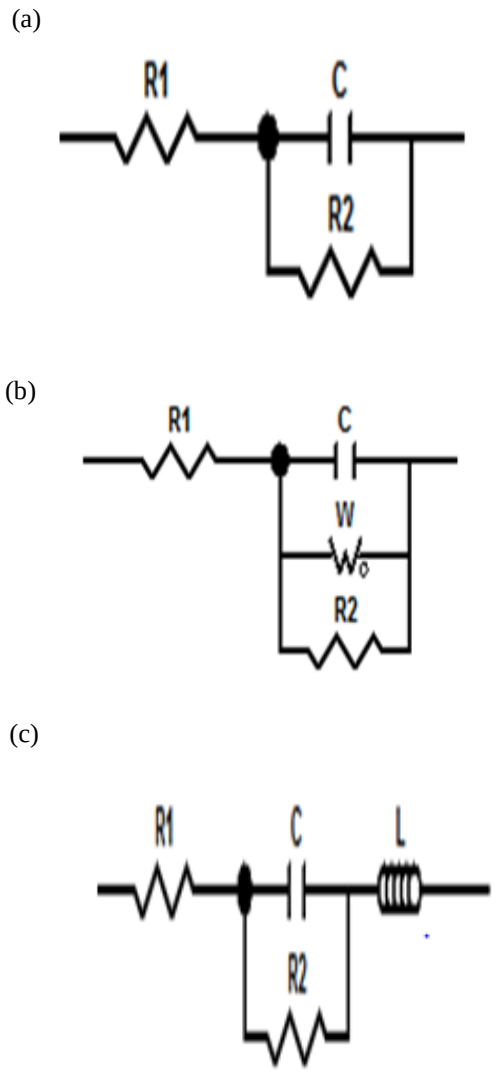

Fig. 5. Equivalent circuits simulating experimental impedance diagrams in Fig. 3.

TABLE II: The resistance of the polarization and the solution in different baths.

Treatment	Al	CAO	SCAO	SAO
R_{po} (ohm)	3838.4	6273.3	5027.9	144.72
R_s (ohm)	14.072	14.072	9.7565	15.141

Experimental impedance spectra were fitted in curves with appropriate equivalent circuits (Fig. 5.). In similar circuits shaw in Fig. 5, R1 is the resistance of the solution, R2 and C the resistance and the capacity of the oxide film or the corrosion product respectively, W and L presented Warburg element and inductor respectively.

Table II groups together the polarization resistances and the solution R_{po} and R_s respectively, the latter being obtained from the adjustment of the equivalent circuits of Fig. 3 to the experimental results. These results show that the aluminum treated with chromic anodic oxidation has a disappearance of the inductance values of the equivalent circuit (Fig. 5 (c)) while the charge transfer resistance R2 has increased with respect to treated or untreated Al with sulfuric anodic oxidation (Fig. 5 (a)) and with respect to the treated cell with sulfo-chromic anodic oxidation which has diffusion (Fig. 5 (b)). In Fig. 3, the results of the adaptation procedure to the experimental data (Nyquist diagrams) clearly confirm this analysis.

4.2 Open circuit potential (OCP)

According to the OCP (Fig. 6), the sample curve treated with CAO at the first point, shows the stabilization during the test time and the fast formation of the passivation layer, which means in parallel the stabilization of the oxide layer formed in an aggressive medium, in the second point, CAO has a higher corrosion potential compared to the sample treated with SCAO, which confirms the noblest of material treated with chromic anodizing. The curve of the aluminum treated with the combination of the two acids shows a decrease of potential as a function of time which means a degradation of the oxide layer formed on the surface of the metal during the time in the same aggressive solution.

4.3 Cyclic voltammetry (single)

Cyclic voltammetry (single) presented in Fig. 7, shows that the behavior of the alloy in an aggressive medium is reacted globally by an activation mechanism. A wide range of passivation is observed at the beginning of the cyclic test (CV) with the three samples treat at different baths (SAO, CAO, SCAO). The depassivation is more pronounced in the case where the aluminum alloy 2024 is treated with sulphuric anodization (SAO), then the one treated with sulfo-chromic anodization (SCAO) and ultimately the alloy that underwent a treatment with chromic anodization (CAO) has a higher corrosion potential compared to previous treatments which confirms the results obtained by EIS.

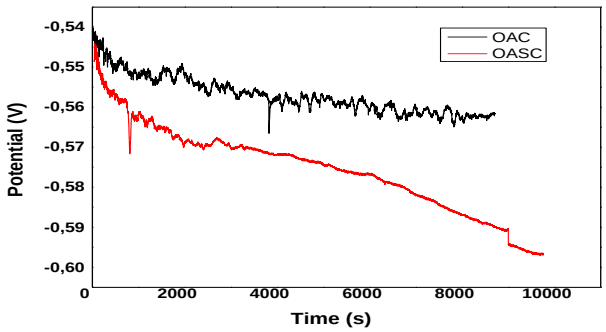

Fig. 6. The OCP curve of AA 2024 treated with different anodizing baths in aerated 3,5% NaCl solution.

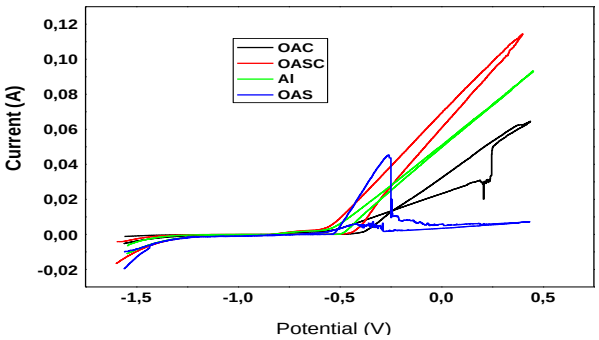

Fig. 7. The cyclic curve of AA 2024 treated with different anodizing baths in aerated 3,5% NaCl solution.

4.4. Surface analysis

SEM images of A2024 alloy with Chromic Anodic Oxidation (CAO) treatment after a day are shown in Fig. 8. This picture shows that the pore distribution is irregular compared to the anodic layers produced in pure Al (Le Coz et al. 2010; Ono et al. 2005), so this surface is characterized by the presence of pores and agglomerations. According to the literature, aluminum alloys are microstructurally characterized, which considerably affects the morphology of the porous anodic layer, which consists of a very tortuous pore network (Zhou et al. 1999). As a result of the EDS analysis (Fig. 10) finds that the surface is composed of aluminum and materials such as copper, oxygen, magnesium and the appearance of a small trace of chromium are shown in table III. More specifically, copper-enriched Al matrices on the substrate surface and incorporation of semiconductor species have also been reported (Zhou et al. 1999; Costenaro et al. 2017). Oxygen bubbles generated by the oxidation of O2 on these semiconductor oxides can both obstruct ion migration (Zhou et al. 1999) and develop pressures of several hundred MPa (Costenaro et al. 2017), leading to uniformity of the thickness of the porous layer (Zhou et al. 1999) and the distribution of stresses inside the anodic film (García-Rubio et al. 2010), respectively.

For this alloy, the corrosion produced appeared compact with some bites, the surface of the treated aluminum had a passive film that contains peaks after being submerged in a high salinity environment causing pitting corrosion that is localized corrosion (Fig. 9). Localized corrosion of AA2024 alloy generally occurs where there are intermetallic particles (Zhou et al. 2012). After that, the corrosion products compacted, which generally prevents corrosion.

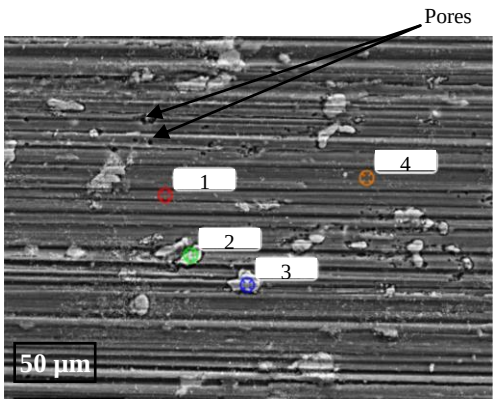

Fig. 8. SEM images of A2024 aluminum alloy treated with Chromic Anodic Oxidation (CAO).

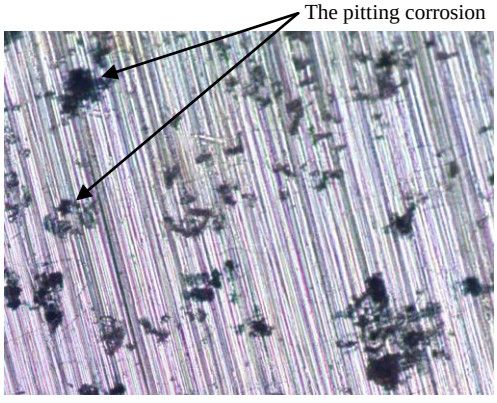

Fig.9. Surface morphology of specimens after Corrosion.

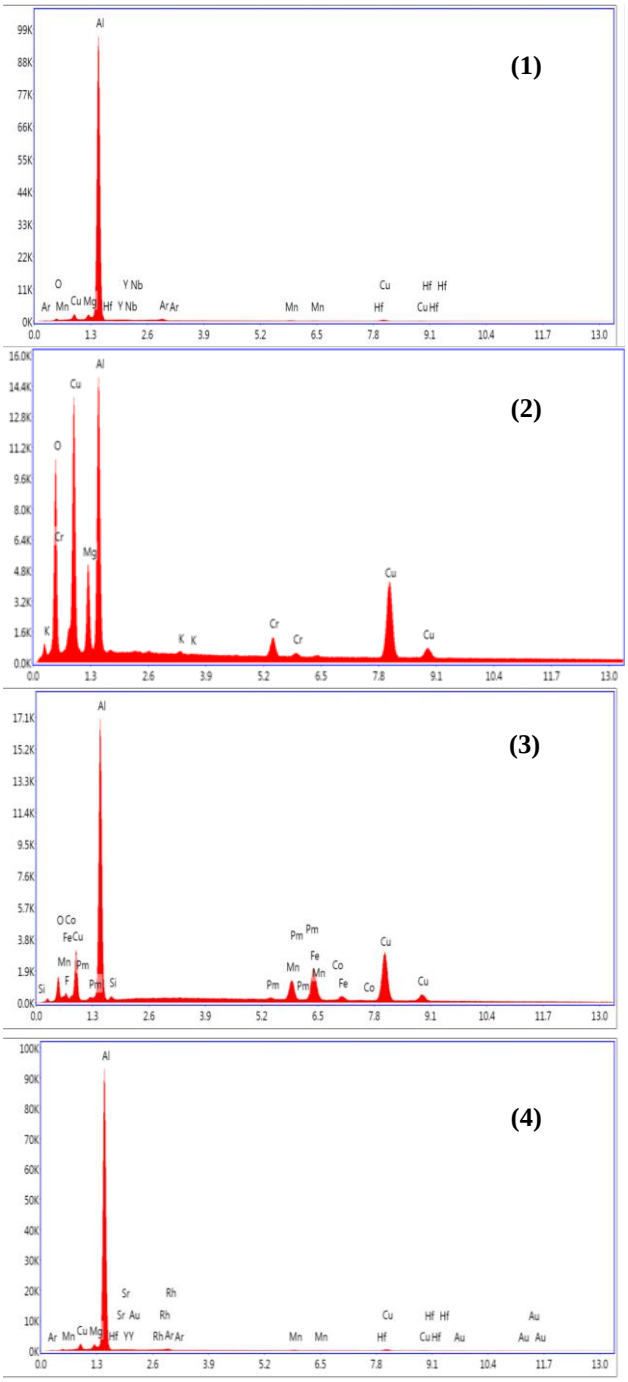

Fig. 10. EDS analysis on the surface of the alloy after surface treatment.

TABLE III: The chemical composition of the oxide layer

Elements	O	Mg	Al	K	Cr	Cu
Weight %	20.37	10.87	27.70	0.12	3.13	37.81
Atomic %	37.38	13.13	30.15	0.09	1.77	17.47
Error %	07.82	08.57	07.58	56.76	5.20	02.60

5. CONCLUSIONS

The anodizing process of 2024-T3 aluminum alloy was performed in an electrolyte of chromic, which was found to be an effective method to improve the corrosion resistance of the aluminum alloy.

Hexavalent chromium conversion coatings are still the conversion layers used today and provide the best protection for 2000 Series alloys against atmospheric corrosion.

Porous type anodization is the case where the electrolytes (chromic acid) chosen have solvent actions on the aluminum substrate and its alloys or on its oxides. The porous oxide layer has characteristics such as resistance to corrosion and wear, high hardness.

Among the advantages of chromatic anodization, it forms an oxide film of small thickness, useful in the case of toleranced parts, which has the advantage of being flexible and has a better rubbing ability than the oxide layers made in a sulfuric medium. Chromic acid does not attack aluminum or alumina, which eliminates any danger in case of retention on molded or assembled parts.

The oxide layer reproduces the structure of the metal and thus the history of the piece. It allows establishing a control health matter, and finally, it allows good adhesion of paint systems.

4. References

Ashtiani, H. R. R and Shahsavari, P. (2016). Strain-dependent constitutive equations to predict high temperature flow behavior of AA2024 aluminum alloy. Mechanics of Materials, 100, 209–218.

Bai, F., Li, J.F., Viehland, D. (2004). Domain hierarchy in annealed (001)-oriented Pb (Mg 1 / 3 Nb 2 / 3) O 3 – x % PbTiO 3 single crystals. Applied Physics Letters, 85, 12.

Costenaro, H., Lanzutti, A., Paint, Y., Fedrizzi, L., Terada, M., de Melo, H.G., Olivier, M.-G. (2017). Corrosion resistance of 2524 Al alloy anodized in tartaric-sulphuric acid at different voltages and protected with a TEOS-GPTMS hybrid sol-gel coating. Surface & Coatings Technology, 324, 438–450.

Datta, J., Samanta, B., Jana, A., Sinha, S., Bhattacharya, C., Bandyopadhyay, S. (2008). Role of Cl^- and NO^-_3 ions on the corrosion behavior of 20% SiC reinforced 6061-Al metal matrix composite: A correlation between electrochemical studies and atomic force microscopy. Corrosion Science, 50, 2658–2668.

De Bonfils-Lahovary, M.L., Josse, C., Laffont, L., Blanc, C. (2019).Influence of hYDROGEN ON the propagation of intergranular corrosion defects in 2024 aluminum alloy. Corrosion Science, 148, 198-205.

Elabar, D., Němcová, A., Hashimoto, T., Skeldon, P., Thompson, G. E. (2015). Effect of sulphate impurity in chromic acid anodizing of aluminium. Corrosion Science, 100, 377–385.

Fadillah, L., Takase, K., Kobayashi, H., Turczyniak-Surdacka, S., Strawski, M., Kowalski, D., Zhu, C., Aoki, Y., Habazaki, H. (2019). The role of tungsten species in the transition of anodic nanopores to nanotubes formed on iron alloyed with tungsten. Electrochimica Acta, 309, 274-282.

García-Rubio, M., Ocón, P., Curioni, M., Thompson, G.E., Skeldon, P., Lavía, A., García, I. (2010). Degradation of the corrosion resistance of anodic oxide films through immersion in the anodising electrolyte. Corrosion Science, 52, 2219–2227.

Jensen, F., Kongstad, I., Dirscherl, K., Gudla, VC., Ambat, R. (2019). High frequency pulse anodising of recycled 5006 aluminium alloy for optimised decorative appearance. Surface & Coatings Technology, 368, 42–50.

Laleh, R. R., Savaloni, H., Abdi, F., Abdi, Y. (2019). Corrosion inhibition enhancement of Al alloy by graphene oxide coating in NaCl solution. Progress in Organic Coatings, 127, 300–307.

Le Coz, F., Arurault, L., Datas, L.. (2010). Chemical analysis of a single basic cell of porous anodic aluminium oxide templates. Materials Characterization, 61, 283–288.

Lee, W and Park, SJ. (2014). Porous Anodic Aluminum Oxide: Anodization and Templated Synthesis of Functional Nanostructures. Chemical reviews, 114, 7487-7556.

Liu, H., Gu, T., Zhang, G., Cheng, Y., Wang, H., Liu, H. (2016). The effect of magneticfield on biomineralization and corrosion behavior of carbon steel induced by iron-oxidizing bacteria. Corrosion Science, 102, 93–102.

Ma, Y., Wen, Y., Li, J., Feng, C., Zhang, Z., Gou, T., Huang, J., Lu, J., Cui, Z., Sun, R. (2020). Fabrication of alumina with ordered tapered-nanopore nested in micro-bowl hierarchical structure by a combined anodization. Materials Chemistry and Physics, 239, 122023.

Moon, S., Nam, Y., Yang, C., Jeong, Y. (2011). Growth of anodic oxide films on AC2A alloy in sulphuric acid solution. Corrosion Science, 53, 1547–1553.

Nettikaden, V. C., Liu, H., Skeldon, P., & Thompson, G. E. (2012). Porous anodic film formation on Al–Ti alloys in sulphuric acid. Corrosion Science, 57, 49–55.

Ono, S., Saito, M., Asoh, H. (2005). Self-ordering of anodic porous alumina formed in organic acid electrolytes. Electrochimica Acta, 51, 827–833.

Palagonia, M.S., Erinmwingbovo, C., Brogioli, D., Mantia, F.L. (2019). Comparison between cyclic voltammetry and differential charge plots from galvanostatic cycling. Journal of Electroanalytical Chemistry, 847, 113170.

Saeedikhani, M., Javidi, M., Vafakhah, S. (2017). Anodising of 2024-T3 aluminum alloy in electrolyte of sulphuric− boric−phosphoric mixed acid containing cerium salt as corrosion inhibitor. Trans. Nonferrous Met. Soc. China 27711−721.

Sousa, C.T., Leitao, D.C., Proenca, M.P., Ventura, J., Pereira, A.M., Araujo, J.P. (2014). Nanoporous alumina as templates for multifunctional applications. Applied Physics Reviews, 1, 3.

Tao, Y., Xiong, T., Sun, C., Jin, H., Du, H., Li, T. (2009). Effect of α-Al_2O_3 on the properties of cold sprayed Al/α-Al_2O_3 composite coatings on AZ91D magnesium alloy. Applied Surface Science, 256, 261–266.

Tao, Y., Xiong, T., Sun, C., Kong, L., Cui, X., Li, T., Song, G.L. (2010). Microstructure and corrosion performance of a cold sprayed aluminum coating on AZ91D magnesium alloy. Corrosion Science, 52, 3191–3197.

Wang, J., Xiong, F., Liu, H., Zhang, T., Li, Y., Li, C., Xia, W., Wang, H., Liu, H. (2019). Study of the corrosion behavior of Aspergillus niger on 7075-T6 aluminum alloy in a high salinity environment. Bioelectrochemistry, 129, 10–17.

Zhang, P and Zu, Y. (2019). Effects of pore parameters on performance of anodic film on 2024 aluminum alloy. Materials Chemistry and Physics, 231, 9–20.

Zhang, S., Zhang, T., He, Y., Feng, Y., Du, X., Ma, B., Zhang, T. (2019). Effect of coastal atmospheric corrosion on fatigue properties of 2024-T4 aluminum alloy structures. Journal of Alloys and Compounds, 802, 511–521.

Zhang, Z., Liu, F., Han, E.H., Xu, L., Uzoma, P.C. (2019). Effects of Al_2O_3 on the microstructures and corrosion behavior of low-pressure cold gas sprayed Al 2024-Al_2O_3 composite coatings on AA 2024-T3 substrate. Surface and Coatings Technology, 370, 53-68.

Zhou, X., Luo, C., Hashimoto, T., Hughes, A.E., Thompson, G.E. (2012). Study of localized corrosion in AA2024 aluminium alloy using electron tomography. Corrosion Science, 58, 299–306.

Zhou, X., Thompson, G. e., Skeldon, P., Wood, G. C., Shimizu, K., Habazaki, H. (1999). Film formation and detachment during anodizing of Al–Mg alloys. Corrosion Science, 41(8), 1599–1613.